Aust. J. Phys., 1985, **38**, 437–48

Electron Microscope Images of Icosahedral and Cuboctahedral (f.c.c. Packing) Clusters of Atoms*

J. C. Barry,[A] *L. A. Bursill*[A] *and J. V. Sanders*[B]

[A] School of Physics, University of Melbourne, Parkville, Vic. 3052.
[B] Division of Materials Science, CSIRO, University of Melbourne, Parkville, Vic. 3052.

Abstract

Images have been computed of closed-shell clusters of 55, 147 or 309 atoms in regular icosahedral and cuboctahedral (f.c.c.) packing for an electron microscope operating at 100 keV, with C_s = 0·7 mm and resolutions of 0·3 and 0·2 nm. The object is to test the possibility of distinguishing the two structures from their images. The results show that sizes and shapes are well represented at optimum defocus but that similar images are often given by both structures. Discrimination could be made for some images at excessive underfocus at 0·2 nm resolution.

1. Introduction

The structures of catalysts are somewhere between those of the translationally periodic crystals of highly ordered atoms, in which lies the appeal of the science of crystallography, and the disordered arrangement of atoms found in glasses and amorphous materials, whose structure is so difficult to describe accurately. Frequently catalysts contain several equally important components, each acting separately. Typically, an active component (Pt, Ni, Pt/Ir as metallic particles, or sulfides MoS_2, WS_2) is dispersed on a less active support of a very high surface area. The highly active component is in the form of very small particles exposing a high ratio of surface to bulk atoms. These particles are kept separate to inhibit sintering by being supported on an oxide of high surface area, often of poor crystallinity. It is important for the catalytic chemist to understand the structures of both components, particularly that of the atoms in the surface. In some other catalytic systems, such as the zeolites, the active component has a well-defined crystallinity, but even here the chemical properties may depend on the presence of a specially incorporated, separate phase (Fe, Co, Ga). A precise knowledge of the size and structure of the metallic particles is essential for a quantitative understanding of these catalysts (Sinfeldt 1969). In this work we are concerned to find out if it is possible to discriminate, in a transmission electron microscope (TEM), between very small clusters of atoms with two different structures.

We consider here the problem of identifying in a TEM clusters of small numbers of atoms packed either as f.c.c. cuboctahedra or as icosahedra. We compute their ap-

* Dedicated to Dr A. McL. Mathieson on the occasion of his 65th birthday.

0004-9506/85/030437$02.00

pearance in a number of principal orientations in a good modern electron microscope in order to find out the reliability of measurements of size and shape, of well-defined small clusters, and to see whether or not there are features in the images which allow the identification of a cluster as icosahedral from its image. Both of these aspects are highly relevant to the examination of metallic particles used as catalysts.

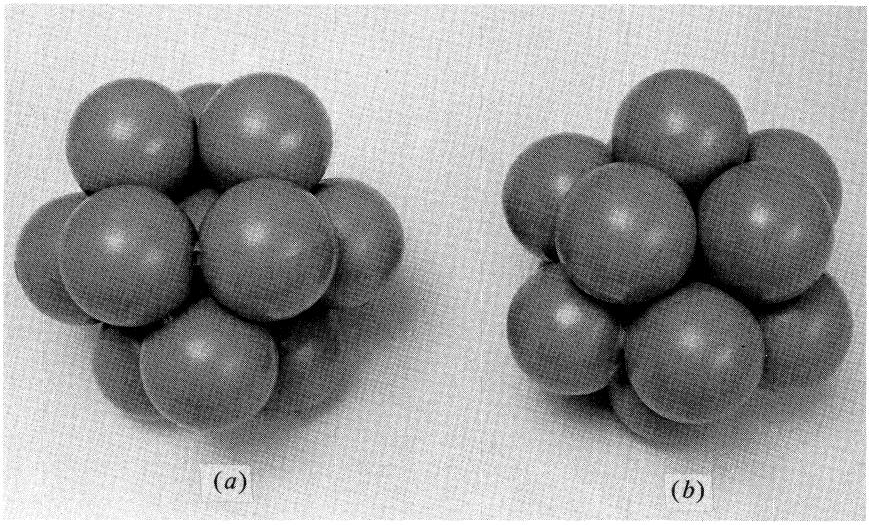

Fig. 1. Photographs of one-shell models of (*a*) the cuboctahedron with f.c.c. packing and (*b*) the icosahedron.

2. Structures of Clusters of Metallic Atoms

When metal atoms which would normally form f.c.c. crystals aggregate from the vapour phase in an inert atmosphere, or in a liquid so that the nucleation is three dimensional, a large proportion of the crystals have shapes which are regular pentagonal biprisms or icosahedra (Kimoto 1979). Their internal structure is found to be a complex arrangement of five or twenty twinned components respectively, and so these structures have become known (Ogawa and Ino 1972) as multiply twinned particles (MTP). Whilst they are found in large numbers in material formed from the vapour in an inert atmosphere, smaller concentrations are found among particles formed by condensation in vacuum onto a surface such as mica or NaCl (Gillett 1977). It is understood that these MTPs grow from a nucleus of four atoms in a tetrahedral arrangement, onto which further growth in the obvious positions in the centres of each face produces very stable non-crystallographic clusters of 7 or 13 atoms which are the precursors of the pentagonal bipyramid and icosahedron respectively (Allpress and Sanders 1970). These shapes can be maintained by the addition of shells of atoms, and for small clusters of atoms are thought to be more stable than a cluster of the same number of atoms with f.c.c. packing (Hoare and Pal 1971, 1972). However, neither arrangement is a lattice structure (Mackay 1962) and as shells are added strain occurs; at some size a rearrangement must occur, with the introduction of some dislocations to produce the MTP of f.c.c. packed components in which each adjacent component

is twin related. Techniques are available for distinguishing the MTP from normal f.c.c. packed crystals in the electron microscope when their size exceeds about 10 nm, and they consist of f.c.c. components (Allpress and Sanders 1967; Yang 1979).

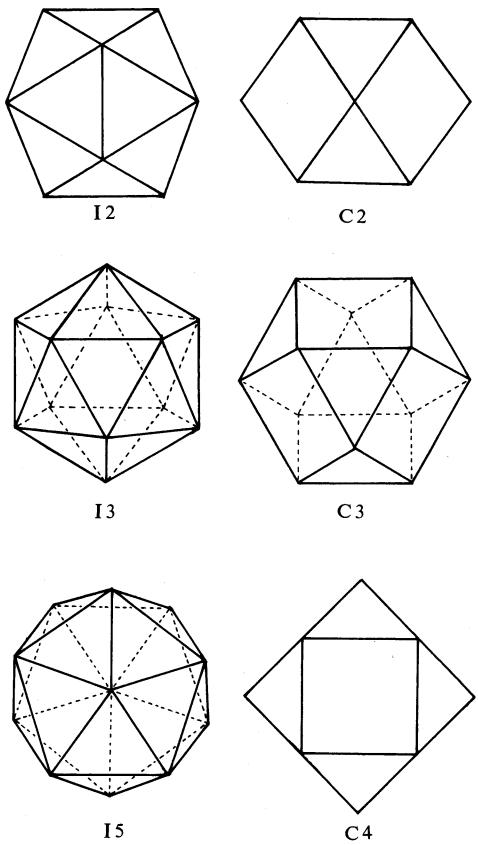

Fig. 2. Projections of icosahedral and cuboctahedral polyhedra, viewed along the 2, 3 and 5 and the 2, 3 and 4 fold axes respectively.

In the size range covered by our computations diffraction patterns are diffuse, but calculations show that it would be possible, in principle, to distinguish an icosahedron because of its distinctive five-fold symmetry in some orientations (Larroque and Brieu 1978). However, the possibility of studying a single particle by diffraction in a standard TEM is remote, but it should be possible in a sophisticated scanning TEM (Howie *et al.* 1982). For TEM examination of the metallic component of a supported catalyst, the metallic particles have no preferred orientation and one would expect their appearance to be sensitive to orientation, at least for larger clusters. The present computations take orientation into account to some extent, but have been restricted to those principal orientations with the electron beam parallel to the 2, 3 and 4 fold axes of the cuboctahedron, and to the 2, 3 and 5 fold axes of the icosahedron. For simplicity these arrangements are written C2, C3 and C4 and I2, I3 and I5 respectively. Fig. 1 shows models of the smallest of the icosahedra and cuboctahedra, and Fig. 2 shows the appearance of projections of polygons of the two structures in the three principal orientations.

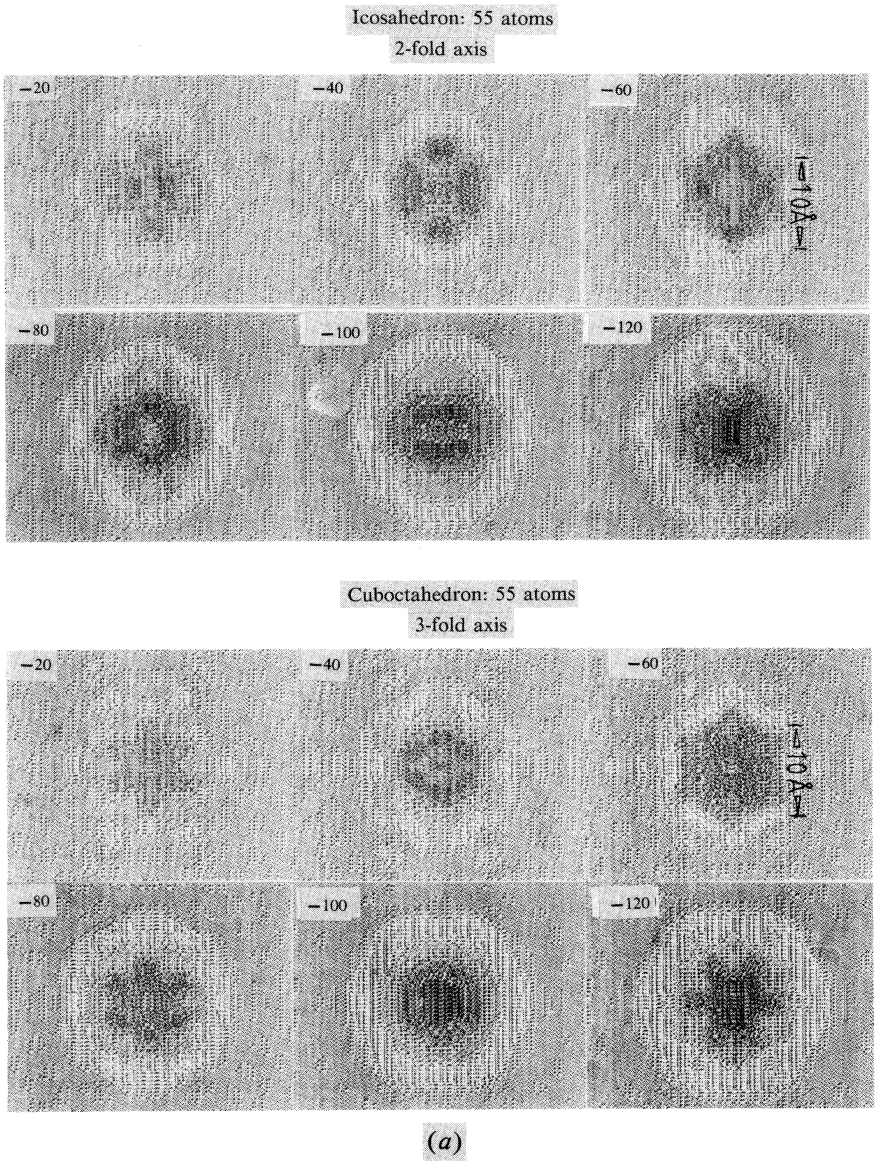

Fig. 3. Effect of variation of the defocus δf on images of icosahedra and cuboctahedra with (*a*) two shells with 55 atoms and (*b*) four shells with 309 atoms for a 100 kV TEM at 0·3 nm resolution. Values of δf (in nm) are shown on each computed image.

3. Computing Methods

The atomic arrangement in the icosahedral cluster is well known (Mackay 1962), and the calculation of the positions of the centres of hard spheres in successive shells is straightforward (Allpress and Sanders 1970). The computations were carried out for silver, where $a_0 = 0{\cdot}40859$ nm, with an interatomic distance for the normal f.c.c.

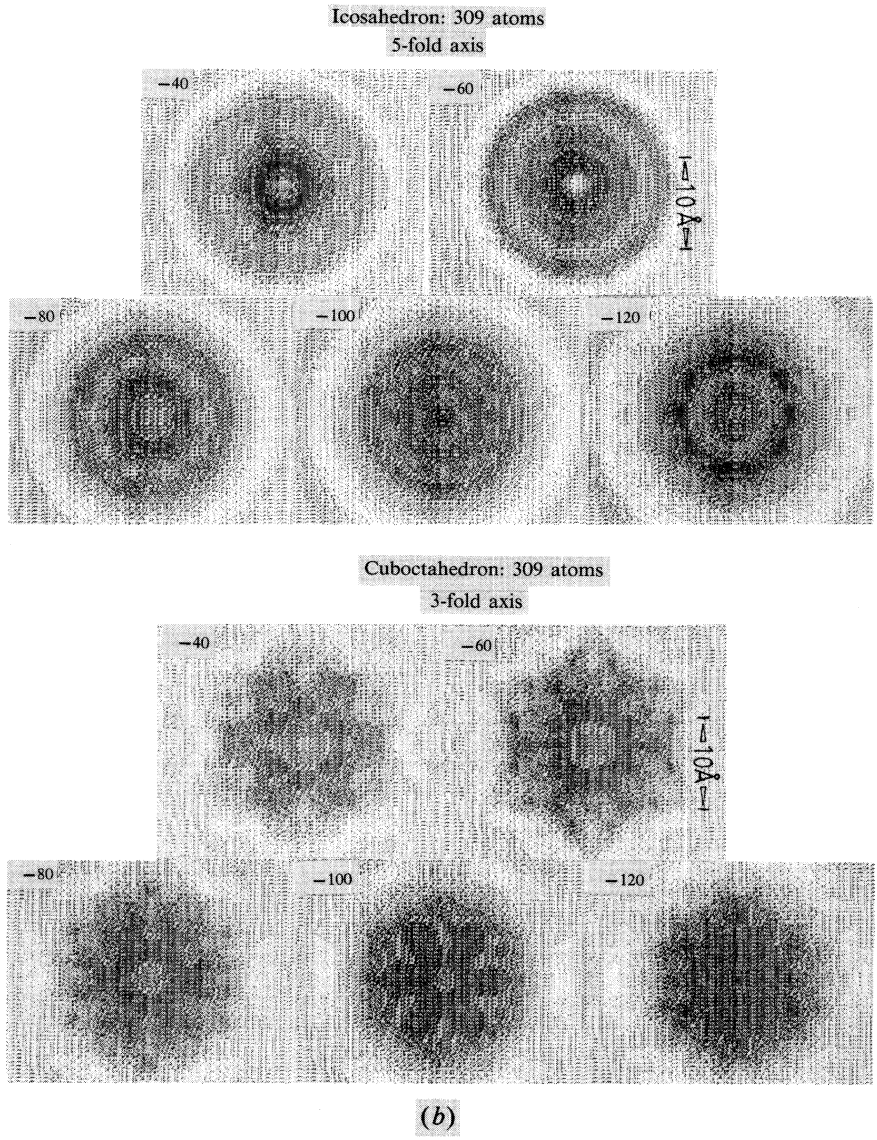

(*b*)

Fig. 3*b*. [*See opposite page*].

structures, equal to the hard sphere diameter, of 0·28892 nm. Atomic positions were calculated for closed shells of 2, 3 or 4 for each structure containing 55, 147 and 309 atoms respectively. No relaxation was allowed (Allpress and Sanders 1970; Burton 1971). The particles have diameters, defined as the size of the circumscribing sphere, of about 1·4, 2·0 and 2·6 nm respectively.

The atomic cluster was placed at the centre of an orthogonal pseudo-cell having dimensions $3{\cdot}2\times4{\cdot}0\ \mathrm{nm}^2$ and made periodic in two dimensions. Multislice com-

putations were carried out in the usual 'periodic-continuation' manner (Grinton and Cowley 1971; Wilson *et al.* 1978/79) for a 100 keV TEM, with $C_s = 0{\cdot}7$ mm, and defocus values δf in the range $-120 \leqslant \delta f \leqslant -20$ nm (the Scherzer optimum defocus is -61 nm). Objective apertures were chosen which limit the image resolution to 0·3 nm for phase contrast, or to 0·2 nm when internal structural detail may appear. The first aperture excludes all the Bragg reflexions from a f.c.c. crystal, because the largest spacing, the 111, is 0·2359 nm, but at 0·2 nm resolution both the 111 and 200 reflections would contribute to the phase contrast image. Some calculations were also carried out for a 500 keV TEM with $C_s = 3{\cdot}3$ mm at a resolution of 0·18 nm.

4. Results

(a) Images at 0·3 nm Resolution

The 0·3 nm resolution phase contrast image shows essentially only the shape of the particle with some Fresnel fringes at the edges, but no internal structure (see Fig. 3). The contrast is very low near gaussian focus, so that in the presence of a little noise, a 55 atom cluster would almost certainly not be detected at $\delta f = -20$ nm. The contrast is enhanced with defocus decreasing through the optimum value $\delta f = -60$ nm. Such behaviour may be used to judge optimum defocus.

Particle size. For catalytic purposes it is important to know if measurements of size can be made reliably from electron micrographs. The apparent diameters of the image as a function of defocus are shown in Table 1, for the two-shell 55 atom

Table 1. Apparent sizes (nm) of clusters of 55 atoms, at 0·3 nm resolution, for various defects of focus δf

δf (nm)	Cuboctahedron			Icosahedron		
	2 fold	3 fold	4 fold	2 fold[A]	3 fold	4 fold
−120	1·44	1·29	1·44	1·67×1·60	1·44	1·29
−100	1·22	1·14	1·44	1·52×1·44	1·44	1·44
−80	1·29	1·22	1·37	1·60×1·37	1·37	1·29
−60	1·22	1·22	1·14	1·44×1·22	1·14	1·22
−40	1·14	1·14	1·14	1·29×1·14	1·29	1·29

[A] This image is quite asymmetric, so that the major and minor dimensions are given.

Table 2. Sizes of clusters of atoms measured on images computed at optimum defocus at 0·3 nm resolution

Atoms in cluster	Cuboctahedron			Icosahedron		
	2 fold	3 fold	4 fold	2 fold	3 fold	5 fold
55	1·22	1·22	1·14	1·44×1·22	1·14	1·22
147	n.c.[A]	n.c.	n.c.	1·90×1·67	1·60	1·67
309	1·90	2·00	2·00	2·28×2·05	2·05	2·13
	Sizes of models of clusters of hard spheres					
55	1·11	1·29	1·11		1·23	
147	n.c.	n.c.	n.c.		1·72	
309	1·92	2·29	1·92		2·71	

[A] Not calculated.

cuboctahedron and icosahedron for the three principal orientations, as well as for $-120 < \delta f < -40$ nm. In most cases the apparent size is a minimum at about optimum defocus ($\delta f = -60$ nm). The apparent size may vary with defocus by up to about 25%. However, a skilful operator should be able to adjust the focus to an optimum value within a much smaller range than that shown in Table 1.

Measurements are given in Table 2 of the apparent sizes of the three sizes of cluster in the principal orientations at optimum defocus, compared with the size of a sphere circumscribing a hard sphere model. In most cases the difference between the sizes of the model and the expected image is less than 10% and about half are within 5%.

Particle shape. The point resolution of a microscope determines the minimum size of a regular polygon of n sides which can be resolved. For a given resolution, this size increases with n in the manner shown by von Borries and Kausche (1940). For this theory, at 0·3 nm resolution, a square and hexagon respectively would be resolved if the circles circumscribing them were greater than 0·91 and 1·015 nm in diameter respectively. All the particles considered here are larger than this, and so their shape should, in principle, be resolvable.

Table 3. Apparent shape of clusters of atoms at 0·3 nm resolution

Square		Hexagonal		Circular	
Cluster	δf (nm)	Cluster	δf (nm)	Cluster	δf (nm)
		309 atoms			
C2	−100	C2	−60	C3	−100
I2	−120	I2	−60	I3	−60
C4	−600	C3	−60	C4	−100
		I3	−80	I5	−60
		55 atoms			
C2	−80	C2	−60	I2	All
C3	−80			C3	All
C4	−60			I3	All
				I5	All

The appearance of the images can be divided into the three classes of square, hexagonal or circular. Table 3 lists the various images with this appearance, and Fig. 4 shows examples. An examination of Table 3 shows that for the 309 atom cluster, the shape alone could not discriminate between I and C, but that for the smallest cluster (55 atoms) a square shape implies a cuboctahedral cluster. However, the diameter of the latter (1·11 nm) is close to the limit of resolution (0·91 nm) and it seems unlikely that these two structures could be distinguished from the shape of their images alone. Fig. 5 shows a pair of through-focus images of a cuboctahedron and an icosahedron, in the condition under which they are most likely to be distinguished.

(b) Images at 0·2 nm Resolution

Internal structure is expected when scattering around the (111) and (200) Bragg reflexions is allowed to contribute to the image. It is of interest to decide if there is additional discrimination of shape, or if the images now become more structure sensitive.

Particle size. The results of a less extensive set of computations (cf. Section 4*a*) are given in Table 4. Thus, at 0·2 nm resolution the images appear to be a little smaller than that of the sphere circumscribing the model.

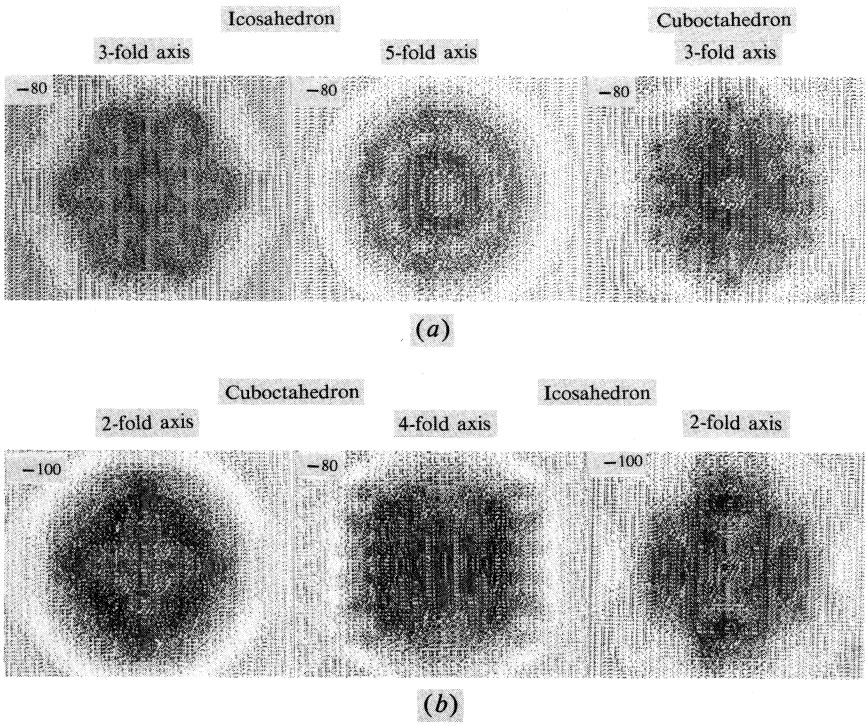

Fig. 4. Examples of different situations producing similarly shaped images for a cluster of 309 atoms at 100 kV and 0·3 nm resolution: (*a*) circular and (*b*) square.

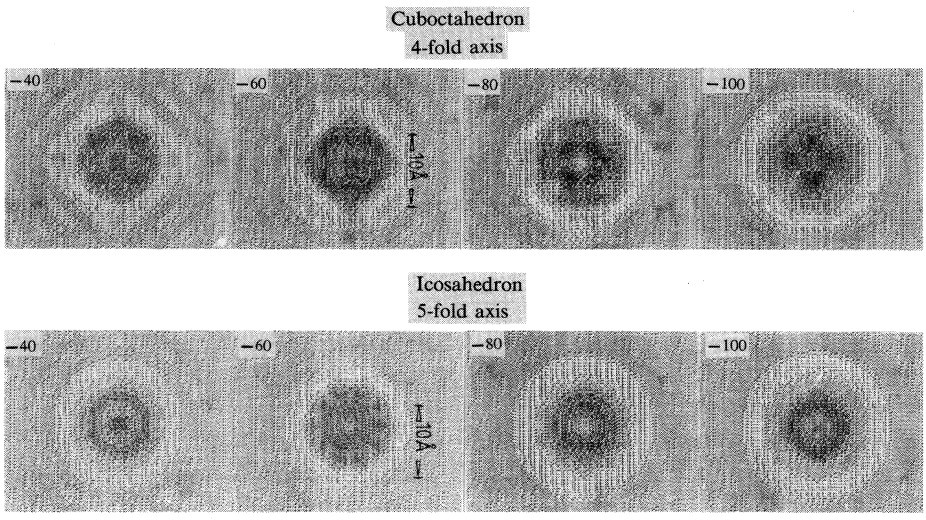

Fig. 5. The most likely situation in which an icosahedral cluster would be distinguished from a cuboctahedron each of 55 atoms at 100 kV and 0·3 nm resolution is from the two through-focal series of a 4-fold and 5-fold axis projection respectively.

Table 4. Apparent sizes of clusters of atoms measured on images computed at optimum defocus at 0·2 nm resolution

Atoms in cluster	Cuboctahedron			Icosahedron		
	2 fold	3 fold	4 fold	2 fold	3 fold	5 fold
55	0·88×1·12	—	—	0·88×1·12	—	—
147	1·62×1·32	—	1·47	—	—	—
309	1·76×2·20	—	—	—	—	—

Particle shape. At 0·2 nm resolution, the diameter of the circles circumscribing the smallest resolvable polygon are 0·6051 and 0·6767 nm for a square and hexagon respectively. This is sufficiently less than the dimensions of the smallest cluster (1·11 nm) that the shapes should be visible. This is shown to be so by the computations. Nevertheless, the smallest clusters (55 atoms) would still probably not be distinguishable at optimum defocus by shape alone (see Fig. 6).

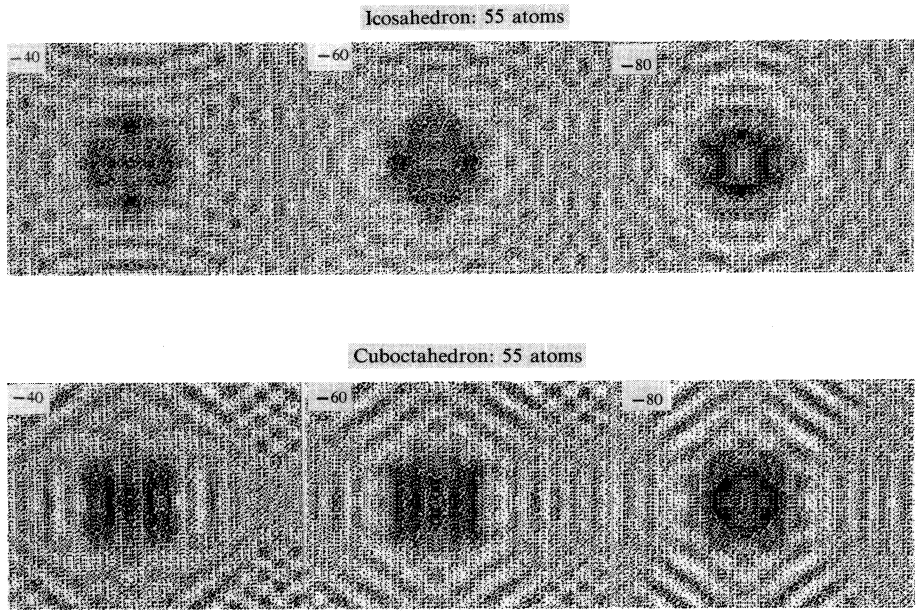

Fig. 6. At 0·2 nm resolution there is fine detail in the form of Fresnel fringes at the edges, and within particles, of 55 atoms. Shown are the icosahedron and cuboctahedron, both for a 2-fold projection at 100 kV and $\delta f = -60$ nm.

(c) Other Means of Discrimination

At 0·2 nm resolution, internal detail becomes apparent in many of the images and fringes outside the cluster are enhanced, particularly at greater underfocus than optimum. The latter detail is an artefact, representing fine structure due to Fresnel fringe effects at the polyhedron–vacuum interface. These fringes may also contribute to fine detail within the image of the particle, since there are facets inclined to the projection axis which will introduce more complex Fresnel effects than are usually considered (Wilson *et al.* 1978/79). Spot contrast in the image, within the particle,

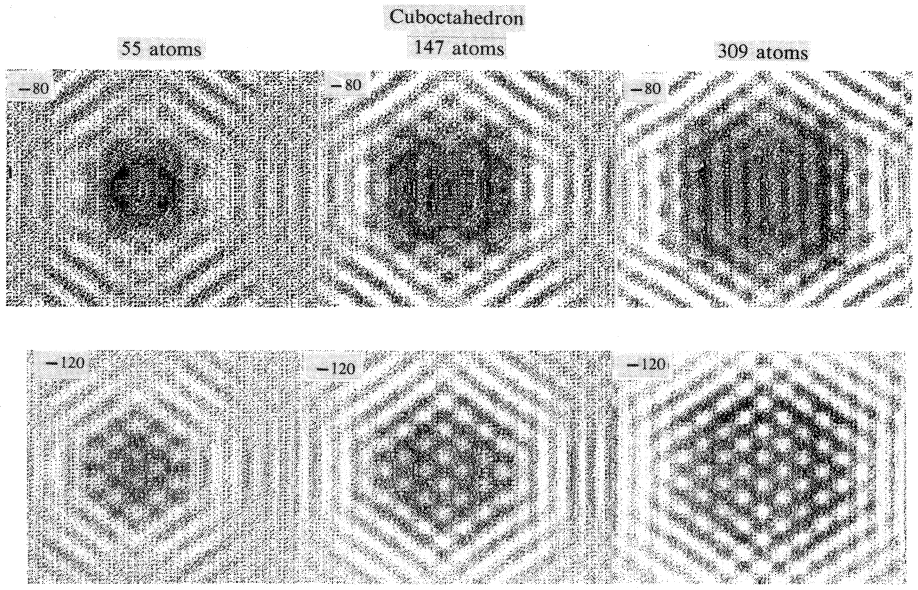

Fig. 7. At 0·2 nm resolution and 100 kV, at excessive defocus ($\delta f = -120$ nm), atomic overlap in projection produces internal detail in images of the cuboctahedron, becoming more apparent with increasing size.

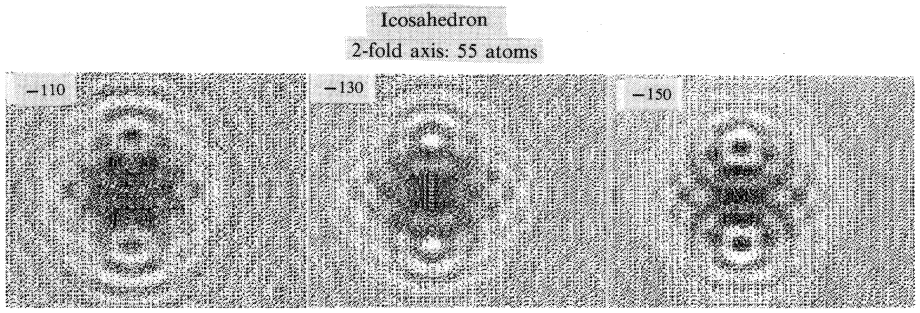

Fig. 8. At 0·2 nm resolution and 100 kV, at excessive defocus, an icosahedral cluster produces a butterfly image, with contrast reversing as δf changes. This is an example for a 55 atom cluster projected down the 2-fold axis.

does not necessarily represent the projected charge density in the object. Thus, white spots within a cluster at $\delta f = -120$ nm correspond not to channels but to the positions of rows of atoms. However, it is atomic overlap in projection which produces this internal detail, which is more apparent in cuboctahedra than in icosahedra. This occurs because in the icosahedra the atoms are not sited as in a lattice, and hence do not necessarily overlap in projection. Thus, the presence of structural detail within the cluster could indicate that it is a f.c.c. structure. For example, in Fig. 7 it can be seen that there is considerable internal detail visible in the cuboctahedron. For larger MTP the atoms have relaxed in position to form a set of twins, each component being a f.c.c. crystal, and again strong projective overlap will occur giving strong structural detail in the images (Marks 1984).

An examination of images at excessive underfocus reveals an additional difference. The icosahedral clusters produce a distinctive set of fringes with the appearance of a butterfly (see Fig. 8), which reverse contrast with a small change of defocus. The cuboctahedra do not produce this effect. It seems possible, therefore, that some icosahedral and cuboctahedral particles could be positively distinguished in underfocus images because of these two distinctive features in these images.

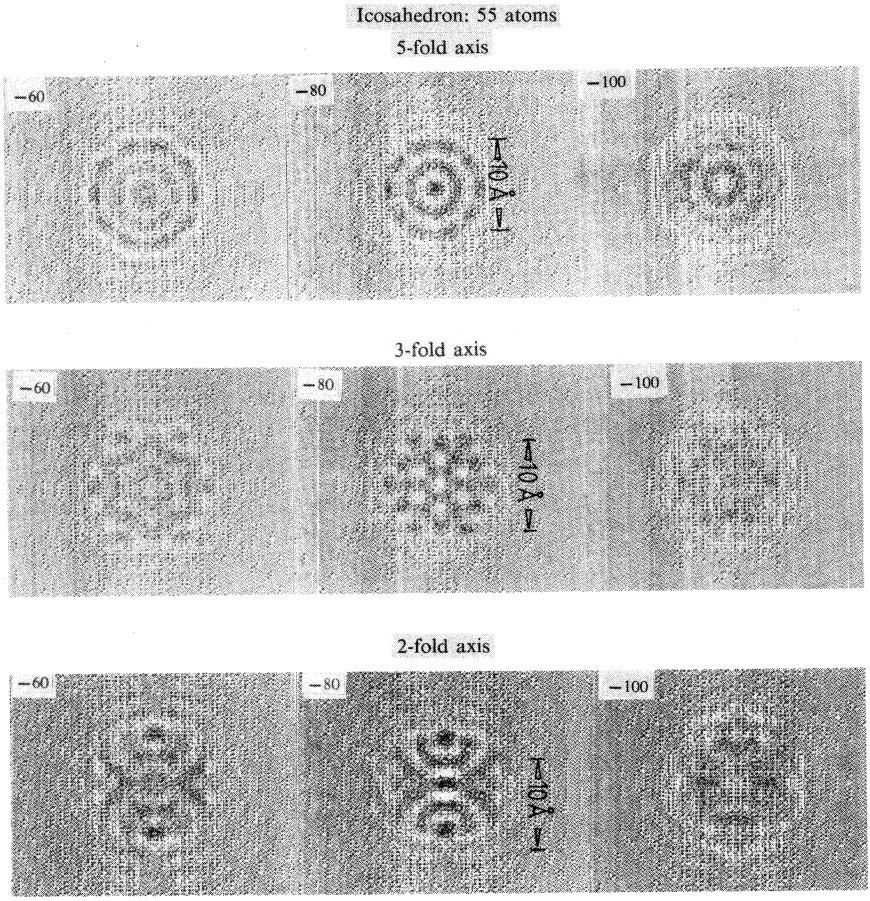

Fig. 9. Examples of images of icosahedral particles, of 309 atoms, viewed down the 2, 3 and 5 fold axes, for the various values of defocus indicated, at 500 kV and 0·18 nm resolution.

(d) Images at 500 kV and 0·18 nm Resolution

Because of the tendency for current and future TEM to use higher voltages for improved resolution, some computations were made for 500 kV and 0·18 nm resolution where 111 and 200 Bragg reflexions would be transmitted through the objective aperture. As expected, more internal detail appears in the smallest clusters. Images down the 5-fold axis appear to show the shell structure in the icosahedral cluster (see Fig. 9). Detail is less clear down the 3-fold axis, but the butterfly fringes appear sharply defined looking down the 2-fold axis. The reversal of contrast occurs between −40 and −80 nm defocus. Again these images indicate that discriminating detail may be more apparent at a rather larger negative defocus than is usually practiced.

5. Discussion

The computed images should give an accurate representation of unsupported particles, such as would be observed at the edge of a fragment of a catalyst support (γAl_2O_3, TiO_2, SiO_2 etc.) projecting over a hole in a carbon support film. This is a realistic situation for practical catalyst examination in a TEM. However, if the particles are viewed through the support, or on a carbon film, the noise and phase-contrast contribution from the support can be expected to modify the appearance of the particle (Kubler *et al.* 1982). However, with the recognition of the possibility of detecting single atoms of tungsten (Iijima 1977), and clusters of three atoms of osmium (Knozinger *et al.* 1981; Schwank *et al.* 1983) on crystalline supports, the shapes of larger clusters might still be detectable.

Our results (Tables 1 and 3) show that the sizes of the particles can be measured reliably on micrographs, mostly to better than 10%. However, in general, whilst the shapes might be resolved, there are sufficient situations where the two types of cluster give similar images under different conditions to make it impossible to discriminate between them without the additional information of the orientation of the cluster, at least at 0·3 nm resolution. At a higher resolution (0·2 nm) some distinctive internal structure and curious contrast effects at excessive underfocus should enable some particles to be positively identified as icosahedra, especially at higher voltages and resolutions better than about 0·18 nm.

Acknowledgment

This work was supported by the Australian Research Grants Scheme.

References

Allpress, J. G., and Sanders, J. V. (1967). *Surf. Sci.* **7**, 1.
Allpress, J. G., and Sanders, J. V. (1970). *Aust. J. Phys.* **23**, 23.
Burton, J. J. (1971). *Nature* **229**, 335.
Gillett, M. (1977). *Surf. Sci.* **67**, 139.
Grinton, G. R., and Cowley, J. M. (1971). *Optik* **34**, 225.
Hoare, M. R., and Pal, P. (1971). *Adv. Phys.* **20**, 161.
Hoare, M. R., and Pal, P. (1972). *Nature* **236**, 35.
Howie, A., Marks, L. D., and Pennycook, S. J. (1982). *Ultramicroscopy* **8**, 163.
Iijima, S. (1977). *Optik* **48**, 193.
Kimoto, K. (1979). *Nippon Kessho Gakkaishi* **6**, 122.
Knozinger, H., Zhao, Y., Tesche, B., Barth, R., Epstein, R., Gates, B. C., and Scott, J. P. (1981). *Faraday Discuss. Chem. Soc.* **72**, 53.
Kubler, O., Downing, K. H., Ruchti, P., and Koller, T. (1982). *J. Microsc. (Oxford)* **125**, 249.
Larroque, P., and Brieu, M. (1978). *Acta Crystallogr.* A **34**, 853.
Mackay, A. L. (1962). *Acta Crystallogr.* **15**, 916.
Marks, L. D. (1984). *Surf. Sci.* **139**, 281.
Ogawa, S., and Ino, S. (1972). *J. Cryst. Growth* **13/14**, 48.
Schwank, J., Allard, L. F., Deeba, M., and Gates, B. C. (1983). *J. Catal.* **84**, 27.
Sinfeldt, J. H. (1969). *Catal. Rev.* **3**, 197.
von Borries, B., and Kausche, G. A. (1940). *Kolloid Z.* **90**, 132.
Wilson, A. R., Bursill, L. A., and Spargo, A. E. C. (1978/79). *Optik* **52**, 313.
Yang, C. Y. (1979). *J. Cryst. Growth* **47**, 274.

Manuscript received 14 December 1984, accepted 25 March 1985